FERMILAB-CONF-06-144-AD

CORRECTION OF UNEVENNESS IN RECYCLER BEAM PROFILE*

J. Crisp, M. Hu, and K.Y. Ng, Fermilab, IL 60510, USA

Abstract

A beam confined between two rf barriers in the Fermilab Recycler Ring exhibits very uneven longitudinal profile. This leads to the consequence that the momentum-mined antiproton bunches will have an intolerable variation in bunch intensity. The observed profile unevenness is the result of a tiny amount of rf imperfection and rf beam-loading. The profile unevenness can be flattened by feeding back the uneven rf fan-back gap voltage to the low-level rf.

INTRODUCTION

Cooled $\bar{p}$ beam stored between two barriers of voltage ± 2 kV inside the Fermilab Recycler Ring exhibits, in general, uneven beam profile. An example is shown in Fig. 1 for a beam of intensity $N_b = 5.1\times 10^{11}$ at $E_0 = 8.939$ GeV, longitudinal emittance $\epsilon_\ell \sim 90$ eVs, rms energy spread $\sigma_E = 3.5$ MeV, and barriers separation $T_2 = 5.8$ μs. The uneven beam profile will lead to $\bar{p}$ bunches of unequal intensities after momentum mining. This will affect the performance of p-$\bar{p}$ collision later in the Tevatron.

The sources of the uneven beam profile can be traced to the rf voltage imperfection and beam-loading at the rf cavities of just a few volts. It takes a rather large number of turns for a particle to drift between the barriers, 1.5×10^5 turns at the energy offset σ_E or 3.5 MeV in this example. Small rf imperfection of, for example, 10 V, will be experienced turn-by-turn and accumulate to produce a total offset as large as ~ 0.31 MeV or 8.8% of σ_E. Sometimes, the profile unevenness can even reach 100% or more. Explicit formula for the accumulated unevenness will be given later.

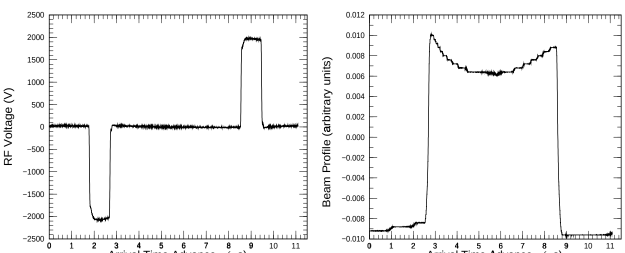

Figure 1: Rf wave (left) and the uneven beam profile (right).

HAISSINSKI EQUATION

Equations of motion of a beam particle of charge $-e$ are

$$\frac{d\tau}{dn} = \frac{|\eta| T_0 \Delta E}{\beta^2 E_0},$$

$$\frac{d\Delta E}{dn} = -|e|V_{\rm rf}(\tau) - e^2 N_b \int_\infty^\tau W_0'(\tau'-\tau)\rho(\tau')d\tau' = -|e|V_{\rm eff},$$

where $\rho(\tau)$ is the linear density or profile of the beam, $T_0 = 11.13$ ns is the revolution period, $\eta = -0.008511$ is the slip factor, βc is the nominal beam velocity with respect to the velocity of light c, $V_{\rm rf}$ is the rf wave, $W_0'(\tau)$ is the longitudinal wake, τ is the arrival time of the particle in advance of some synchronous particle, and the revolution turn n has been chosen as the independent variable. The Hamiltonian can be written as

$$H = -\frac{|\eta| T_0 \sigma_E^2}{\beta^2 E_0}\left[-\frac{\Delta E^2}{2\sigma_E^2} - \frac{|e|\beta^2 E_0}{|\eta| T_0 \sigma_E^2}\int_0^\tau V_{\rm eff}(\tau')d\tau'\right].$$

When a Gaussian distribution in energy offset is assumed, the particle density in the longitudinal phase space becomes

$$\psi(\Delta E, \tau) \sim \exp\left[-\frac{\Delta E^2}{2\sigma_E^2} - \frac{|e|\beta^2 E_0}{|\eta| T_0 \sigma_E^2}\int_0^\tau V_{\rm eff}(\tau')d\tau'\right].$$

Integration over ΔE gives the linear density

$$\rho(\tau) = \rho(0)\exp\left[-\frac{|e|\beta^2 E_0}{|\eta| T_0 \sigma_E^2}\int_0^\tau V_{\rm eff}(\tau')d\tau'\right].$$

The profile unevenness thus arises from the exponent

$$\frac{|e|\beta^2 E_0}{|\eta| T_0 \sigma_E^2}\int_{\tau_1}^{\tau_2} V_{\rm eff}(\tau')d\tau' = \frac{\tau_2 - \tau_1}{\Delta\tau}\frac{e\bar{V}_{\rm eff}}{\sigma_E},$$

where

$$\bar{V}_{\rm eff} = \frac{1}{\tau_2 - \tau_1}\int_{\tau_1}^{\tau_2} V_{\rm eff}(\tau')d\tau',$$

and $\Delta\tau = |\eta| T_0 \sigma_E / (\beta^2 E_0)$ denotes the drift of the particle at energy offset σ_E in one revolution. It is easy to see

1. Constant $V_{\rm eff}$ leads to a roughly linear beam profile.
2. If $V_{\rm eff}$ is sinusoidal, the integration in $V_{\rm eff}$ should be performed over the half-wavelength $\lambda/2$, so that

$$\text{Unevenness} = \frac{\lambda/2}{\Delta\tau}\frac{\bar{V}_{\rm eff}|_{\lambda/2}}{\sigma_E},$$

which is what we postulated in the previous section.

3. The profile unevenness will be larger for a longer beam confined between two barriers. The unevenness becomes more significant when the beam is cooled since σ_E becomes smaller and so does the drift $\Delta\tau$ per revolution. These predictions have been verified in observation.
4. For a sinusoidal rf bucket, the synchrotron period is very much shorter, for example, ~ 100 turns in the Tevatron. Thus an rf imperfection and beam-loading of 10 V will lead to a beam profile variation of ~ 0.5 keV only, which is negligibly small compared with the energy spread of the beam.

EFFECTS OF BEAM-LOADING

If there is no rf imperfection, $V_{\rm eff}$ receives contribution in between the two confining barriers only from the impedance around the ring. The Recycler impedance comes mostly from the rf cavities and is mostly real with $R_s \approx 130\ \Omega$. Since the wake function is $W_0'(\tau) = R_s\delta(\tau)$, the profile between barriers can be simplified to

$$\rho(\tau) = \rho(0)\exp\left[-\alpha_R N_b \int_0^\tau \rho(\tau')d\tau'\right],$$

* Work supported by U.S. Department of Energy

with $\alpha_R = e^2\beta^2 E_0 R_s/(|\eta| T_0 \sigma_E^2)$. The Haissinski equation can be converted into a differential equation

$$\frac{d\rho(\tau)}{d\tau} = -\alpha_R N_b \rho^2(\tau)$$

between the two barriers with the solution

$$\rho(\tau) = \frac{\rho(0)}{1+\alpha_R N_b \tau\rho(0)},$$

where $\tau\rho(0)$ varies from 0 at the tail of the bunch to ~ 1 at the head. Thus beam profile is linear only if $\alpha_R N_b \ll 1$.

For the beam in Fig. 1, $\alpha_R N_b = 0.081$. Since $\tau\rho(0) = 0$ at the tail and ~ 1 at head, the beam profile is roughly linear, about 8% higher at tail than at head, or leaning backward. Such a left-right asymmetry of the longitudinal beam profile is rather common in electron bunches, where particles are creeping ahead because electron machines are mostly above transition ($\eta > 0$). Here $\eta < 0$ and the beam leans backward instead.

The beam-loading voltage is $V_{\rm bl} \approx |e| N_b R_s / T_2 = 1.83$ V. We see that such a small voltage has been magnified through turn-by-turn accumulation to a 8% unevenness or 0.28 MeV. Since we see more than a linear slanting beam profile in Fig. 1, there must also be rf imperfection between the two barriers.

EFFECTS OF RF IMPERFECTION

The rf gap voltage $V_{\rm eff}$ in Fig. 1 experienced by the beam is integrated to arrive at the rf potential well depicted in Fig. 2 with a magnified view shown on the right. We see that the well bottom is not flat, is not linearly slanting, but has a curvature. The unevenness is just $\sim 1.4\%$ of the depth of the well. A flat well bottom will lead to a flat beam profile, a linear slanting well bottom will lead to a linear beam profile, and a well bottom with curvature will lead to a beam profile with curvature. If we study the curvature of the well bottom more closely, we find that it closely resembles the negative of the beam profile curvature in Fig. 1. This is not accidental. As will be shown below, the two curvatures are in fact proportional to each other when the profile unevenness is small.

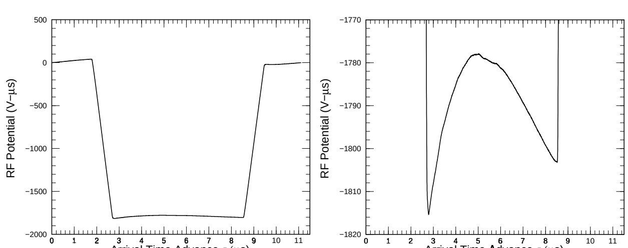

Figure 2: The rf potential well corresponding to the rf gap voltage $V_{\rm eff}$ in Fig. 1. A magnified view is shown on the right.

Using the imperfect rf well bottom, the beam profile can be computed from the Haissinski equation using suitable normalization. The result is plotted in red in Fig. 3, which agrees with the measured beam profile from Fig. 1. This indicates that our understanding of the profile unevenness is correct and the assumption of a Gaussian energy-offset distribution is acceptable.

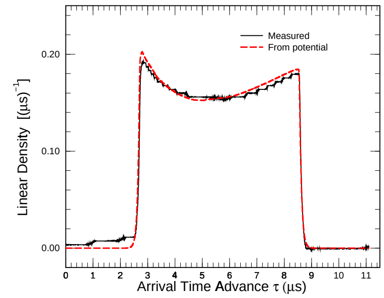

Figure 3: (Color) Beam profile computed from the rf fan-back voltage $V_{\rm eff}$ (red) agrees very well with the measured beam profile (shown in black).

CRITERION OF REQUIRED FLATNESS

A tolerable fractional unevenness in profile F implies

$$\left|\frac{e\beta^2 E_0}{|\eta| T_0 \sigma_E^2}\int_0^\tau V_{\rm eff}(\tau')d\tau'\right|_{\rm max} < F.$$

In other words, the allowable unevenness in rf potential-well bottom must satisfy

$$\left|\int_0^\tau V_{\rm eff}(\tau')d\tau'\right|_{\rm max} < \frac{|\eta| T_0 \sigma_E^2}{e\beta^2 E_0} F.$$

In this particular example, an unevenness in potential well of $|\int V_{\rm eff} d\tau|_{\rm max} = 37$ V-μs will lead to a maximum profile unevenness of $F = 0.28$. If the tolerable profile unevenness is only $F = 10\%$, the rf imperfection must be compensated to the extent that the integrated unevenness of rf potential-well bottom becomes less than 13 V-μs.

Since out of the total $\left|\int V_{\rm eff} d\tau\right|_{\rm max} = 37$ V-μs only 0.08 V-μs comes from beam-loading, rf imperfection is dominating here. However, the $\bar{p}$ beam in the Recycler is intended to be very much stronger reaching $N_b = 3\times 10^{12}$ in the future; the wake term may become more dominating then. Thus the total profile unevenness will become very much larger in the future and unevenness compensation cannot be avoided in operation.

UNEVENNESS COMPENSATION

Method 1

The easiest compensation of profile unevenness is to feedback to the low-level rf (LLRF) the negative of the fan-back cavity gap voltage $V_{\rm eff}$ (Fig. 4).

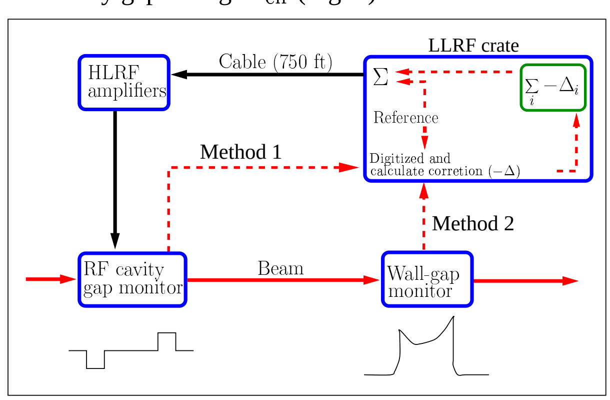

Figure 4: (Color) Block diagram showing correction to the beam profile unevenness through feedback. The rf fan-back gap voltage (Method 1) or the beam profile picked up by the wall-gap monitor (Method 2) is digitized, processed, compared with the reference, converted to suitable voltage table, and fedback to the LLRF.

In the present example, $V_{\rm eff} \sim 32$ V at the tail of the beam and -9.2 V at the head. Amplification from the LLRF to the cavity gap is 2000. Feedback at the LLRF is therefore -16 mV at tail and $+4.6$ mV at head. To avoid phase-space increase, the feedback has to be applied slower than one synchrotron period of the beam, ~ 1.7 s here at $1\ \sigma_E$. Thus the feedback has to be applied in many small steps (more than 10) in practice.

At the rf fan-back, 1.6 V out of the ± 2 kV barrier voltage is only 0.08%, pretty small, and the signal-to-noise ratio is therefore very low. In practice, we need to average over 200 to 500 data samples in order to sort out the signals. With a 1 GHz oscilloscope, the time required is typically ~ 1 min, including data storage and processing.

Method 2

Another compensating method is to employ the beam profile unevenness picked up at wall-gap monitor as feedback input. Because the profile unevenness is very much larger than the rf imperfection, the signal-to-noise ratio is relatively very much higher, so that an average of ~ 20 sets of readout will be enough. But there are other disadvantages. The Haissinski equation can be expanded as

$$\rho(\tau) \approx \rho(0) \left[1 - \frac{|e|\beta^2 E_0}{|\eta| T_0 \sigma_E^2} \int_0^\tau V_{\rm eff}(\tau')d\tau'\right].$$

Thus profile unevenness is

$$\Delta\rho(\tau) = \rho(\tau) - \rho(0) = \frac{|e|\beta^2 E_0}{|\eta| T_0 \sigma_E^2}\, \rho(0) \int_0^\tau V_{\rm eff}(\tau')d\tau',$$

and is proportional to rf potential-well unevenness, a property we noticed earlier. The compensation voltage is

$$V_{\rm comp} = -\frac{|\eta| T_0 \sigma_E^2}{|e|\beta^2 E_0} \frac{\Delta\rho'(\tau)}{\rho(0)}. \qquad (1)$$

The compensation procedure involves a differentiation and a multiplication with a constant which depends on the energy-offset distribution. For a distribution with a smooth spread at both ends, the dependency should be small. This method also involves an expansion by omitting all higher-order terms. However, this last concern can be eliminated by solving the Haissinski equation exactly with the solution given by Eq. (1) but with $\rho(0)$ replaced by $\rho(\tau)$.

EXPERIMENTAL IMPLEMENTATION

The fan-back voltage was recorded with a Tektronix TDS 3054B digital oscilloscope, with time resolution 2 ns. The data were averaged for 500 samples to further improve signal-to-noise ratio. The noisy data were first low-pass filtered to remove high-frequency noises. A decimation was made to fit the 18.936-ns time resolution of the input table to be applied to the LLRF. The correction pulse was then sent to the LLRF in small steps.

As a test, a proton beam with modest intensity 1×10^{11} and $\sigma_E \sim 2$ MeV is stored in a barrier bucket of length 2 μs. The profiles before and after correction are shown in Fig. 6.

In another example shown in Fig. 7, the first compensation removed the curvature of the beam profile but leaving behind a slanting profile. This is because the rf pulses are ac-coupled to the beam and $\int V_{\rm eff} d\tau \neq 0$ between the barriers. Further voltage fine adjustment was then made to ensure $\int V_{\rm eff} d\tau = 0$ and the beam profile became flat.

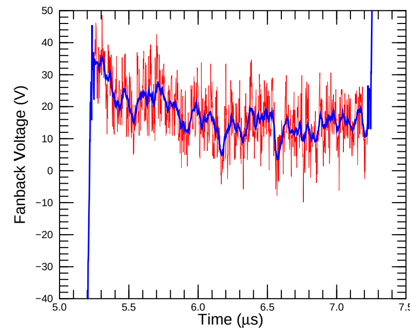

Figure 5: (Color) The signals at 2 ns interval was low-pass filtered, and then decimated to fit the 18.936-ns LLRF time resolution table.

Figure 6: (Color) A proton beam with profiles before (left) and after (right) profile-unevenness compensation.

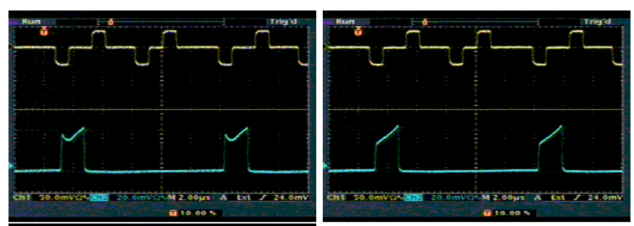

Figure 7: (Color) First compensation removed beam profile curvature leaving behind a slanting profile, since $\int V_{\rm eff} d\tau \neq 0$. Fine adjustment of the barrier voltage was required to totally flatten the uneven profile.

SUMMARY

The connection between the uneven beam profile and rf imperfection and beam-loading has been given. The compensation of beam-profile unevenness has been successfully performed. Although compensation is straight forward, it is rather tedious because the compensation has to be applied in many small steps to avoid phase-space increase. When the area under the fan-back voltage is nonzero, fine-adjustment of the barrier wave must be performed. To guarantee a correction pulse free of any dc component, a simple solution is to compute the difference between $V_{\rm eff}$ and the reference voltage over the *entire* revolution period (not just between the barriers) when determining the feedback to the LLRF. An automation of the compensation procedure has been designed and is being built, hoping that the compensation could be performed in the future by just pushing a button.